Proc. Natl. Acad. Sci. USA
Vol. 92, pp. 6469–6473, July 1995
Neurobiology

Illusory contours activate specific regions in human visual cortex: Evidence from functional magnetic resonance imaging

JOY HIRSCH†‡§, ROBERT L. DELAPAZ¶, NORMAN R. RELKIN§, JONATHAN VICTOR§, KARL KIM†§, TAO LI†, PETER BORDEN†, NAVA RUBIN‖, AND ROBERT SHAPLEY**

Departments of †Neurology, and ¶Radiology, Memorial Sloan–Kettering Cancer Center, New York, NY 10021; §Department of Neurology and Neuroscience, Cornell University Medical College, New York, NY 10021; ‖Department of Psychology, Harvard University, Cambridge, MA 02138; and **Center for Neural Science, New York University, New York, NY 10003

Communicated by James E. Rothman, Memorial Sloan–Kettering Cancer Center, New York, NY, January 3, 1995 (received for review December 19, 1994)

ABSTRACT **The neural basis for perceptual grouping operations in the human visual system, including the processes which generate illusory contours, is fundamental to understanding human vision. We have employed functional magnetic resonance imaging to investigate these processes noninvasively. Images were acquired on a GE Signa 1.5T scanner equipped for echo planar imaging with an in-plane resolution of 1.5 × 1.5 mm and slice thicknesses of 3.0 or 5.0 mm. Visual stimuli included nonaligned inducers (pacmen) that created no perceptual contours, similar inducers at the corners of a Kanizsa square that created illusory contours, and a real square formed by continuous contours. Multiple contiguous axial slices were acquired during baseline, visual stimulation, and poststimulation periods. Activated regions were identified by a multistage statistical analysis of the activation for each volume element sampled and were compared across conditions. Specific brain regions were activated in extrastriate cortex when the illusory contours were perceived but not during conditions when the illusory contours were absent. These unique regions were found primarily in the right hemisphere for all four subjects and demonstrate that specific brain regions are activated during the kind of perceptual grouping operations involved in illusory contour perception.**

Our goal is to identify areas of human cortex involved in the operation of perceptual grouping of local features into a global percept. We used functional magnetic resonance imaging (fMRI), a noninvasive neuroimaging technique which relies on local variations in blood supply and O_2 concentration during neural activity (1–3), to investigate these processes. Neural activation within the cerebral cortex is believed to be associated with an increase in blood flow that is out of proportion to the O_2 consumption, thus decreasing the capillary O_2 extraction fraction and delivering more oxyhemoglobin to the local venous circulation (4–7). The resulting decrease in the local capillary and venous deoxyhemoglobin concentration results in an increase in the T2* weighted magnetic resonance signal due to the decreased paramagnetic effects of deoxyhemoglobin (8, 9). These local changes in blood chemistry can be observed without the use of exogenous contrast enhancing agents on clinical magnetic resonance scanners (3, 10–12), which has enabled fMRI localization of visual (10–16), motor (3, 17–19), auditory (20), speech (21), taste (22), and olfactory (23) processing in the human brain. Since fMRI is now established as a method for exploring the functional organization of the human brain (24), we applied this technique to investigate the global processes of perceptual grouping in vision.

Borders between visual objects and their background are usually defined by changes in luminance or color. However, perceptual borders can be created by inducing elements distant from the perceived border, as in Kanizsa's triangle (25). The phenomena of perceived visual borders not associated with net luminance or color changes across the border are collected under the heading of anomalous or illusory contours (we use the latter term). Though termed illusory, such contours arise in nature and are of perceptual significance in signaling the occlusion of one surface by another (25). The neural mechanisms that produce the perception of illusory contours are crucial for normal image segmentation mechanisms and the active creation of the perceptual representation of visual surfaces. Since illusory contours are also a specific example of the general phenomenon of the global perceptual grouping of local image features, the neural mechanisms involved here will reveal much about the properties of grouping mechanisms that are needed for global form perception (26, 27).

The view that illusory contours reveal mechanisms of normal form perception is often, though not exclusively, associated with the "bottom-up" or physiological view of the contour-detecting mechanisms as being hardwired neural mechanisms that are excited involuntarily by any visual pattern. This view has gained support from experiments that indicate that there are physical limits to the spatial range of interpolation in illusory contours (28) and that manipulation of stimulus parameters like contrast and color contrast can prevent contours from being seen in situations in which a cognitive solution should be possible (25). Also, von der Heydt, Peterhans, and Baumgartner (29–31) have shown that some cells in the Macaque monkey's secondary visual cortical area, V2, respond to illusory contours in a way that resembles human visual perception. More recently, Grosof *et al.* (32) found evidence for responses to illusory contours in V1, the earliest cortical stage of visual signal processing. Related work on spatial linking of local information in macaque V1 by Lamme *et al.* (33) and Purpura and Victor (34) indicates that perceptual grouping may begin already in V1. These neurophysiological results led us to investigate the illusory contours and perceptual grouping in human cerebral cortex with fMRI.

METHODS AND RESULTS

Images were acquired on a 1.5-tesla magnetic resonance scanner (General Electric) that was retrofitted for echo planar imaging (Advanced NMR Instascan) located in the Department of Radiology at Memorial Sloan–Kettering Cancer Center. A gradient echo sequence [echo time (TE) = 60 ms; repetition time (TR) = 3 s; flip angle = 30°] and a standard quadrature head coil were employed to acquire T2*-weighted

The publication costs of this article were defrayed in part by page charge payment. This article must therefore be hereby marked "*advertisement*" in accordance with 18 U.S.C. §1734 solely to indicate this fact.

Abbreviations: fMRI, functional magnetic resonance imaging; voxel, the smallest unit of volume sampled.

‡To whom reprint requests should be addressed.

images with an inplane resolution of 1.56 × 1.56 mm (128 × 256 matrix; 20 × 40 cm field of view). Four healthy subjects with no history of vision-related complaints participated in the experiment: subject A, right handed male; subject B, left handed male; subject C right handed male; and subject D, right handed female. Handedness was determined by the Edinburgh handedness inventory (35). Slice thickness was either 3.0 mm (subject B) or 5.0 mm (subjects A, C, and D) and either 12 (subjects A, B, and C) or 16 (subject D) contiguous axial slices were acquired simultaneously. On the basis of a midsagittal view of a T1 image of the brain for each subject, slice positions were selected for the T2* image to cover the occipital lobe. For subjects A, B, and C, the slices were parallel to the anterior-to-posterior commissure (AC/PC) line (36), and for subject D, the slices were horizontal (approximately parallel to the canthomeatal line). Light levels inside the scanner room were dim, and lights inside the scanner were off for subjects A and B.

Five kinds of visual stimuli were employed: (*i*) pacmen inducers positioned as if on the corners of a square but misaligned, such that no illusory contour was generated (Fig. 1 *A* and *B*); (*ii*) pacmen inducers in the identical positions but aligned, such that an illusory Kanisza square was formed (Fig. 1 *C* and *D*); (*iii*) a real square either with (Fig. 1*E*) or without (Fig. 1*F*) the pacmen; (*iv*) simple bullets along the vertical or horizontal meridians for retinotopic mapping; and (*v*) a fixation mark alone. All line segments and stimulus objects were white on a dark background. The presentation order of conditions varied across subjects, and all subjects were familiar with the stimuli prior to the experiment. Subjects viewed the stimuli through a slanted mirror incorporated into the head coil and located above the head. The stimuli were back projected onto a screen located at the foot of the scanner platform. Viewing distance from eye to center screen was 355 cm, and the stimulus field subtended approximately 6° × 6° of visual angle. The intersecting line segments of the fixation mark (crosshair) subtended 0.8° of visual angle. This crosshair was presented alone and also on all stimuli. Two forms of the pacmen were employed: solid pacmen (Fig. 1 *B* and *D*), and lined pacmen (Fig. 1 *A* and *C*). Each individual pacman subtended approximately 2.0° of visual angle in diameter, the centers of the pacmen were separated by 4.5° along the horizontal and vertical direction and were separated from the crosshair by 3.2°. Stimuli were flickered at a rate of approximately 4 Hz with a duty cycle of 50% for subjects A, C, and D; no flicker was used for subject B.

Two identical image acquisition runs, each lasting either 90 s and consisting of 30 images or 120 s and consisting of 40 images, were performed for each condition. The two independent runs were used in the coincidence analysis (see below). The initial 10 images (30 s) of each run were acquired during baseline (resting) conditions, the following 10 images (30 s) were acquired during visual stimulation, and the final 10 or 20 images (30 s or 60 s) were acquired during a poststimulation (recovery) resting condition. Because of afterimages following the stationary stimulus for subject B, 40 images were acquired on each run, and the recovery baseline period was taken as the final 10 images. Baseline data consisted of images 2–10, the stimulation period consisted of images 12–20, and the poststimulation (recovery) consisted of images 22–30 (subjects A, C, and D) or images 32–40 (subject B). To avoid the onset and offset latency periods (8), images 11, 21, and 31 were excluded from the analyses, and image 1 was excluded because of signal transients due to the absence of prior magnetization (10). Prior to statistical analysis, all brain images for each subject were computationally aligned (37), and a two-dimensional inplane boxcar or Gaussian filter was applied to each image. The smallest unit of volume sampled, the voxel, therefore, represented a centroid of activation.

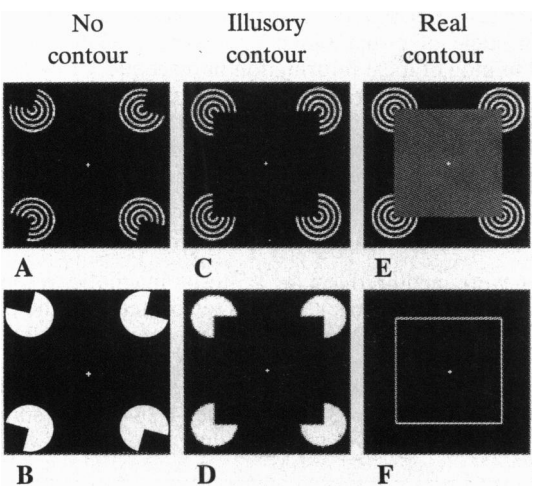

FIG. 1. Illustrations of the contour stimuli for which functional data were acquired.

A multistage statistical technique was used to determine the activation of each voxel in the image: stage 1, comparison of mean baseline and stimulation signals; stage 2, comparison of mean stimulation and recovery baseline signals; and stage 3, coincidence analysis by comparison of activation on two independent runs (38). The empirical probability of a voxel passing all three stages of the analysis was determined by calculations based on images acquired from a "phantom," a 12-cm-diameter plastic sphere filled with a dilute solution of copper sulfate (General Electric standard). The phantom provides an empirical estimate of the influence of statistical and instrumental factors on the level of confidence. Statistical stages 1, 2, and the coincidence requirement were applied to imaging data obtained from a phantom, and the empirical probability that a voxel passed all stages was found to be ≤0.0008. No clusters of significant voxels either within a slice or across slices were observed in the phantom data. In the human experiments, many more than 0.0008 of the voxels passed the criteria, and voxels deemed activated by these criteria were often clumped within and across slices.

The multistage analysis was performed for all conditions. In the illustrations to follow, voxels which were activated in response to stimuli shown in Fig. 1 *C* and *D* (illusory contours) are colored yellow. Red indicates voxels which were activated in response to stimuli shown in Fig. 1 *A* and *B* (no contour), and blue indicates voxels activated in response to stimuli shown in Fig. 1 *E* and *F* (real contours). Six contiguous axial slices with the activity-related voxels (slices 2–7) for subject A are shown in Fig. 2. Slice 2 is the most inferior, and numbers (upper right) of corresponding slices increment superiorly in 5-mm steps. Note that the right side of the brain (indicated as R) is shown on the left side of the images according to the clinical convention. The occipital cortex is on the bottom of each slice. The regions of interest described below meet the criteria of multiple contiguous voxels in plane with continuing activity across adjacent slices.

Several general observations can be made. First, the illusory-contour-related activity (yellow) and the no-contour-related activity (red) tend to overlap the same posterior locations on slices 2 (both hemispheres), 3 (right hemisphere), 4 (right hemisphere), and 7 (right hemisphere). The illusory-contour-related activity is generally more extensive than the real- or no-contour-related activity. The posterior location on the right hemisphere of slice 6 is the area with the most distinct illusory-contour-alone activity. It adjoins a similar region on slice 5, which is also activated by the real contour, suggesting a common locus of processing for the contour, whether real or perceptually generated.

The crosshair alone activity (indicated by the arrows on slices 4 and 5 of Fig. 2) indicates the locations of the regions

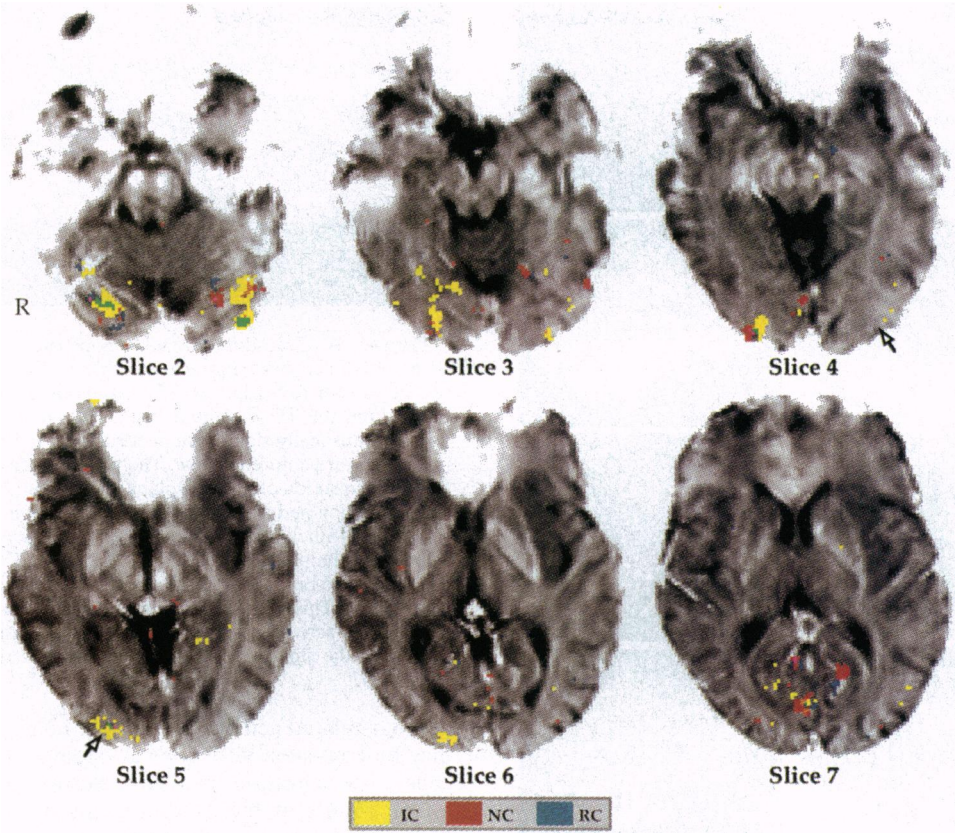

FIG. 2. Activated voxels for each condition (slices 2–7 for subject A) are identified by color: yellow, illusory contour (IC); red, no contour (NC); and blue, real contour (RC). Areas of overlap are indicated by mixtures of the above colors. Slice 2 is most inferior, and all slices are contiguous. A boxcar filter (±2 voxels) was applied prior to statistical analysis. The base grey-scale image is the average of all 180 T2*-weighted images for each voxel. Image left is brain right (indicated by R), image top is frontal brain, and image bottom is posterior brain. Arrows on slices 4 and 5 indicate locations of activation associated with central fixation of the crosshair alone.

that correspond to the central fixation stimulus. Therefore, the more medial areas of activity shared by all three conditions on slice 4 can be assumed to represent the peripheral pacmen common to all stimuli. The approximate location of the boundaries of Brodmann's areas 17/18 and 18/19 were identified by the responses to the vertical and horizontal meridian stimuli, respectively (39–41). Activity related to the vertical meridian bullets coincided with much of the slice 2 activity as well as the medial regions of slice 6. Activity related to the horizontal meridian bullets coincided with a subset of activity on slices 3, 4, and 7. These landmarks suggest that the distinct illusory-contour-alone activity observed on slice 6 is within extrastriate and, in particular, Brodmann's area 18 for subject A.

A distinct illusory-contour-alone region was located in the right hemisphere for all subjects as shown in Fig. 3. The color code is the same as described for Fig. 2. The location of each axial slice is indicated by the red line on the corresponding midsagittal view. These single slices were selected to illustrate that specific occipital–cortical regions associated with illusory contour perception were predominantly located within the right hemisphere. However, as in Fig. 2, these regions were multifocal, and individual differences were observed. Note that no real contour condition was run on subject B and that the real contour stimulus for subject D did not include pacmen. These experimental differences may account for some of the variation among the four subjects. Expected variations in brain size and morphology (42–44), as well as small differences in slice angles, further contribute to the different appearances of these slices and activation patterns. Nonetheless, all subjects consistently demonstrated clustered, right-hemisphere, illusory-contour-alone activity. As in the case of subject A, the illusory-contour-alone regions were contiguous with activity on adjacent slices, and adjacent slices also indicated the presence of real contour activity for all subjects who ran that condition. The clustered responses strengthen the confidence levels of the findings (45). Although subject A was the only subject for which responses to both the horizontal and vertical meridians were obtained, responses to the vertical meridians (subjects B and C) and crosshair alone (subjects B and D) suggest that the unique illusory contour activity is in extrastriate regions of the visual cortex for these subjects as well. A three-dimensional reconstruction of all the brain slices imaged in subject A is shown in Fig. 4 and illustrates the extensive regions of visual cortex activated in response to illusory contours.

DISCUSSION

The perception of illusory contours is an example of a perceptual grouping process in human vision. Here, we are presenting evidence for cortical activation associated with such contour perception in the human visual system by using fMRI. Results from four subjects demonstrated that the illusory-contour stimuli (Fig. 1 *C* and *D*) generated fMRI responses distinct from the responses to the no-contour stimuli (Fig. 1 *A* and *B*). These no-contour stimuli were identical to the illusory-contour stimuli, except that the orientation of the inducers (pacmen) was varied, such that perceptual integration into a single shape bounded by illusory contours was impossible. We conclude that the areas activated when the subject perceived a unified shape and illusory contours represent the activity of a population of neurons associated with the process of grouping local features via perceptual contours.

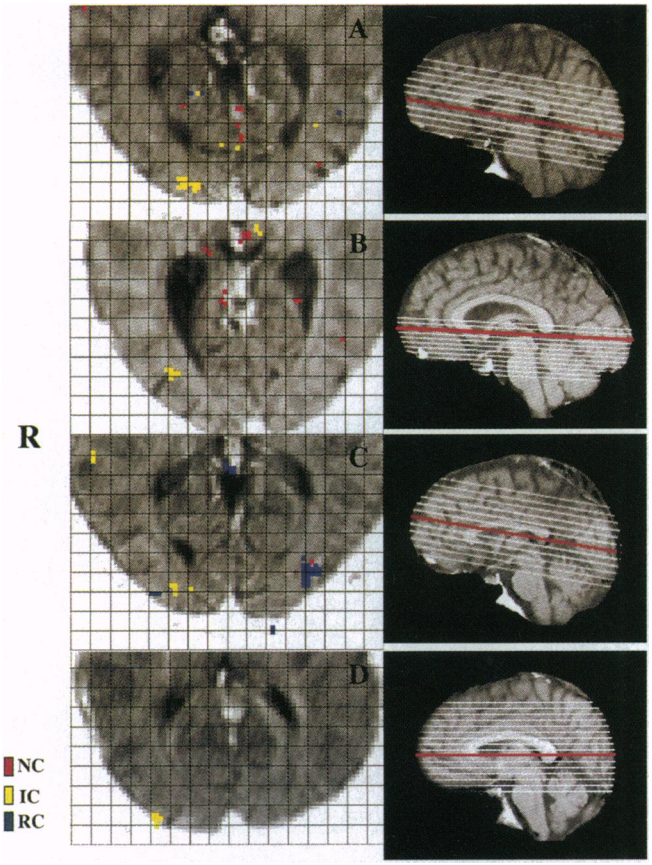

FIG. 3. A representative slice for each subject illustrates the visual regions associated with the illusory-contour (IC) stimulus (yellow). Red and blue indicate active regions associated with no-contour (NC) and real-contour (RC) conditions, respectively. Right brain is designated by "R". The grid is the sampling matrix where each box contains a 5 × 5 array of pixels. The center locations of the acquired slices are indicated by the parallel lines shown on the corresponding midsagittal views from the T1-weighted images. Slice positions were selected to cover the inferior occipital lobe, and slices for subjects A, B, and C were oriented parallel to and on the anterior-to-posterior commissure line. The plane orientation for subject D was horizontal. Slice thickness was 5.0 mm for all subjects except for subject B, where the slice thickness was 3.0 mm. The red line indicates the location of the axial slice shown on the left.

Stimuli along the vertical and horizontal meridians and located at the fixation point served as functional markers for the approximate boundaries between Brodmann's areas 17/18 and 18/19, as well as the foveal representation. Comparison of these landmark responses with those of the most prominent illusory-contour-related responses places the location of the distinct illusory-contour-related activation in extrastriate regions for all subjects. However, the neuroanatomical locations for the illusory-contour-alone activity occur in multiple foci and may also include foci not resolved by our analysis. In particular, these observations do not rule out striate cortex as a participant in contour-related activity. For example, the medial and anterior (right hemisphere) regions shown on slice 6 (subject A; Fig. 2) are near the vertical meridian regions of activity and may implicate striate cortex involvement. For subject C, the vertical-meridian-related activity coincided with illusory-contour-related activity on slices 2, 4, 5, and 8–10, and for subject B, the illusory-contour- and vertical-meridian-related activity coincided on slices 3, 4, 6, and 11. To the extent that the vertical meridian serves as a landmark for the area 17/18 border, these coincident illusory contour and vertical meridian regions may suggest striate activity in contour-related processes. All subjects showed a predominance of illusory-contour-related activity in the right hemisphere. This finding may be consistent with clinical findings showing right hemisphere specialization for figural closure tasks (46, 47).

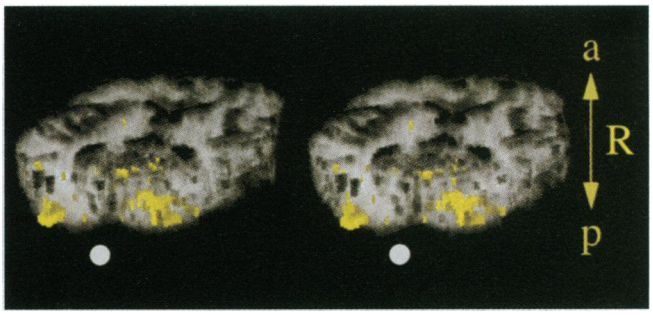

FIG. 4. A three-dimensional reconstruction of all echo-planar slices and of activation patterns of subject A in response to an illusory square as shown in Fig. 1*D*. The voxels of the base images of brain tissue from the T2*-weighted image are colored grey; the activated voxels (statistically significant according to the procedures described in the text) are colored yellow. The three-dimensional image shown is the reconstruction of six echo-planar slices (Fig. 2). Three-dimensional reconstruction and rotation of viewing direction was done with VOXEL VIEW on a Silicon Graphics computer. The two views shown are directed at the posterior surface of the brain. The images are rotated 7° to facilitate binocular fusion into a three-dimensional stereo image of the brain. This allows the reader to appreciate more fully the extent of the brain activated by the illusory-contour stimulus. Also, one can scrutinize the image to see the bias towards right (R) hemisphere activation.

The results of these experiments do not rule out either higher level or lower level processes in the formation of illusory contours or in perceptual grouping (25). While our findings are consistent with a data-driven, bottom-up approach to illusory-contour perception, the effect of activity in other brain areas may modulate the responses in areas that we have observed. It is also possible that, in addition to activating distinct regions, illusory-contour responses may potentiate or diminish local responses to the inducing features at early levels of cortical image processing or may cause overt linking activity.

Drs. Ronald A. Castellino, Chairman, Department of Radiology, Memorial Sloan–Kettering Cancer Center; Jerome B. Posner, Chairman, Department of Neurology, Memorial Sloan–Kettering Cancer Center; and Fred Plum, Chairman, Department of Neurology and Neuroscience, New York Hospital–Cornell Medical Center, generously supported the many phases of this research. We are grateful to Aries Arditi, Richard Everson, and Kathy McKay for significant contributions to the development of this project in addition to serving as subjects. Tom White contributed to the computational and analysis systems, and Karina Tulipano, Charles G. Nyman, Kyoung-Min Lee, Jody Cramm, and Bradley Beattie provided computational and technical support. Preliminary reports of the general statistical technique were presented at the 1994 annual meeting of the Society for Magnetic Resonance. This project was funded by the Memorial Sloan–Kettering Cancer Center and Sloan–Kettering Institute (J.H. and R.D.); a William T. Morris Foundation Fellowship (K.K.); National Institutes of Health Grants EY7977 (J.V.) and EY1472 (R.S.); the C. V. Starr Foundation, A. L. Aitken, and the Lookout Foundations (N.R.R.).

1. Ogawa, S., Lee, T.-M., Nayak, A. S. & Glynn, P. (1990) *Magn. Reson. Med.* **14,** 68–78.
2. Turner, R., Bihan, D. L., Moonen, C. T. W., Despres, D. & Frank, J. (1991) *Magn. Reson. Med.* **22,** 156–166.
3. Kwong, K., Belliveau, J., Chesler, D., Goldberg, I., Weisskoff, R., Poncelet, B., Kennedy, D., Hoppel, B., Cohen, M., Turner, R., Cheng, H.-M., Brady, T. & Rosen, B. (1992) *Proc. Natl. Acad. Sci. USA* **89,** 5675–5679.
4. Roy, C. & Sherrington, C. (1890) *J. Physiol. (London)* **11,** 85–108.
5. Plum, F., Posner, J. & Troy, B. (1968) *Arch. Neurol.* **18,** 1–13.
6. Posner, J., Plum, F. & Poznak, A. (1969) *Arch. Neurol.* **20,** 388–396.

7. Fox, P. T., Raichle, M. E., Mintun, M. A. & Dence, C. (1988) *Science* **241,** 462–464.
8. Ogawa, S., Menon, R., Tank, D., Kim, S.-G., Merkle, H., Ellermann, J. & Ugurbil, K. (1993) *Biophys. J.* **64,** 803–812.
9. Shulman, R. G., Blamire, A. M., Rothman, D. L. & McCarthy, G. (1993) *Proc. Natl. Acad. Sci. USA* **90,** 3127–3133.
10. Bandettini, P., Wong, E., Hinks, R., Tikofsky, R. & Hyde, J. (1992) *Magn. Reson. Med.* **25,** 390–397.
11. Ogawa, S., Tank, D. W., Menon, R., Ellermann, J. M., Kim, S.-G., Merkle, H. & Ugurbil, K. (1992) *Proc. Natl. Acad. Sci. USA* **89,** 5951–5955.
12. Turner, R., Jezzard, P., Wen, H., Kwong, K. K., Bihan, D. L., Zeffiro, T. & Balaban, R. S. (1993) *Magn. Reson. Med.* **29,** 277–279.
13. Belliveau, J., Kennedy, D., McKinstry, R., Buchbinder, B., Weisskoff, R., Cohen, M., Vevea, J., Brady, T. & Rosen, B. (1991) *Science* **254,** 716–719.
14. Blamire, A., Ogawa, S., Ugurbil, K., Rothman, D., McCarthy, G., Ellermann, J., Hyder, F., Rattner, Z. & Shulman, R. (1992) *Proc. Natl. Acad. Sci. USA* **89,** 11069–11073.
15. Schneider, W., Noll, D. C. & Cohen, J. D. (1993) *Nature (London)* **365,** 150–153.
16. Engel, S., Rumelhart, D., Wandell, B., Lee, A., Glover, G., Chichilnisky, E.-J. & Shadlen, M. (1994) *Nature (London)* **369,** 525.
17. Kim, S.-G., Ashe, J., Hendrich, K., Ellermann, J. M., Merkle, H., Ugurbil, K. & Georgopoulos, A. P. (1993) *Science* **261,** 615–617.
18. Schad, L. R., Trost, U., Knopp, M. V., Muller, E. & Lorenz, W. J. (1993) *Magn. Reson. Imaging* **11,** 461–464.
19. Constable, R., McCarthy, G., Allison, T., Anderson, A. & Gore, J. (1993) *Magn. Reson. Imaging* **11,** 451–459.
20. Binder, J., Ralo, S., Hammeke, T., Yetkin, F., Jesmanowicz, A., Bandettini, P., Wong, E., Estkowski, L., Goldstein, M., Haughton, V. & Hyde, J. (1994) *Ann. Neurol.* **35,** 662–672.
21. Hinke, R. M., Hu, X., Stillman, A. E., Kim, S.-G., Merkle, H., Salmi, R. & Ugurbil, K. (1993) *NeuroReport* **4,** 675–678.
22. Hirsch, J., DeLaPaz, R. L., Relkin, N., Victor, J., Li, T. & Kim, K. (1994) *Soc. Neurosci. Abstr.* **20,** 1474.
23. Koizuka, I., Yano, H., Nagahara, M., Mochizuki, R., Seo, R., Shimada, K., Kubo, T. & Nogawa, T. (1994) *ORL* **56,** 273–275.
24. Cohen, M. S. & Bookheimer, S. Y. (1994) *Trends Neurosci.* **17,** 268–277.
25. Petry, S. & Meyer, G. (1987) *The Perception of Illusory Contours* (Springer, New York).
26. Gibson, J. J. (1966) *The Senses Considered as Perceptual Systems* (Houghton Mifflin, Boston).
27. Marr, D. (1982) *Vision* (Freeman, New York).
28. Shapley, R. & Gordon, J. (1987) in *The Perception of Illusory Contours*, ed. Petry, S. & Meyer, G. (Springer, New York).
29. Heydt, R. v. d., Peterhans, E. & Baumgartner, G. (1984) *Science* **224,** 1260–1262.
30. Heydt, R. v. d. & Peterhans, E. (1989) *J. Neurosci.* **9,** 1731–1748.
31. Peterhans, E. & Heydt, R. v. d. (1989) *J. Neurosci.* **9,** 1749–1763.
32. Grosof, D. H., Shapley, R. M. & Hawken, M. J. (1993) *Nature (London)* **365,** 550–552.
33. Lamme, V. A. F., van Dijk, B. W. & Spekreijse, H. (1993) *Nature (London)* **363,** 541–543.
34. Purpura, K. P. & Victor, J. D. (1994) *Proc. Natl. Acad. Sci. USA* **91,** 8482–8486.
35. Oldfield, R. (1971) *Neuropsychologia* **9,** 97–113.
36. Talairach, J. & Tournoux, P. (1988) *Co-planar Stereotaxic Atlas of the Human Brain* (Thieme Medical Publishers, New York).
37. Woods, R. P., Mazziotta, J. C. & Cherry, S. R. (1993) *J. Comput. Assisted Tomogr.* **17,** 536–546.
38. Hirsch, J., DeLaPaz, R. L., Relkin, N., Victor, J., Li, T., Kim, K., White, T. & Olyarchuk, J. (1994) *Soc. Magn. Reson. Imaging Abstr.* **637.**
39. Horton, J. C. & Hoyt, W. F. (1991) *Arch. Ophthalmol.* **109,** 816–824.
40. Horton, J. C. & Hoyt, W. F. (1991) *Brain* **114,** 1703–1718.
41. Clarke, S. & Miklossy, J. (1990) *J. Comp. Neurol.* **298,** 188–214.
42. Damasio, H. & Damasio, A. (1989) *Lesion Analysis in Neuropsychology* (Oxford Univ. Press, New York).
43. Steinmetz, H. & Seitz, R. J. (1991) *Neuropsychologia* **29,** 1149–1161.
44. Rademacher, J., Caviness, J., Steinmetz, H. & Galaburda, A. (1993) *Cereb. Cortex* **3,** 313–329.
45. Friston, K., Worsley, K., Frackowiak, R., Mazziotta, J. & Evans, A. (1994) *Hum. Brain Mapping* **1,** 210–220.
46. Lezak, M. D. (1983) *Neuropsychological Assessment* (Oxford Univ. Press, New York).
47. Wasserstein, J., Zappulla, R., Rosen, J., Gerstman, L. & Rock, D. (1987) *Brain Cognition* **6,** 1–14.